NASA Technical Memorandum 83746

Optical and Other Property Changes of M-50 Bearing Steel Surfaces for Different Lubricants and Additives Prior to Scuffing

James L. Lauer and Norbert Marxer
Rensselaer Polytechnic Institute
Troy, New York

and

William R. Jones, Jr.
Lewis Research Center
Cleveland, Ohio

Prepared for the
Joint Lubrication Conference
cosponsored by the American Society of Mechanical Engineers
and the American Society of Lubrication Engineers
San Diego, California, October 22-24, 1984

NASA

OPTICAL AND OTHER PROPERTY CHANGES OF M-50 BEARING STEEL SURFACES FOR DIFFERENT LUBRICANTS AND ADDITIVES PRIOR TO SCUFFING*

James L. Lauer and Norbert Marxer
Rensselaer Polytechnic Institute
Troy, New York 12181

and

William R. Jones, Jr.
National Aeronautics and Space Administration
Lewis Research Center
Cleveland, Ohio 44135

SUMMARY

An ester lubricant base oil containing one or more standard additives to protect against wear, corrosion, and oxidation was used in an experimental ball/plate elastohydrodynamic contact under load and speed conditions such as to induce scuffing failure in short times. Both the ball and the plate were of identically treated M-50 steel. After various periods of operating time the wear track on the plate was examined (i) with an interference microscope of ±30 Å depth resolution and (ii) sometimes also with a scanning ellipsometer and (iii) an Auger spectrometer. The optically deduced surface profiles varied with wavelength, indicating the presence of surface coatings, which were confirmed by the other instruments. As scuffing was approached, a thin (~100 Å) oxide layer and a carbide layer formed in the wear track in particular when tricresylphosphate antiwear additive was present in the lubricant. The rates of the formation of these layers and their reactivity toward dilute alcoholic HCl depended strongly on the lubricant and additives. Based on these results suggestions for improved formulations and a test method for bearing reliability could be proposed.

INTRODUCTION

In earlier work (refs. 1 and 2) with an optical profilometer we showed that preceding scuffing failure the wear track of M-50 steel bearings operated under elastohydrodynamic or mixed lubrication became more reactive toward hydrochloric acid. Microscopic changes of the optical surface profile were used as measures of reactivity. The presence or absence of tricresylphosphate additive in the lubricating oil would have considerable influence on the profiles of the bearing surfaces even before exposure to the hydrochloric acid probe. Furthermore our studies showed that TCP in a lubricant reduced bearing traction significantly after soaking. In a related study Faut and Wheeler (ref. 3) showed that the friction of TCP-lubricated M-50 bearings would be

*This work was sponsored by a grant from NASA Lewis Research Center, Grant NAG 3-222. Additional funding was provided by the Air Force Office of Scientific Research, Grant No. AFOSR-81-0005 and by a grant from the Army Research Office, Grant No. DAAG 2483K0058.

reduced by 30 to 50 percent when the contact temperature exceeded a critical value in the neighborhood of 218° C, the exact temperature depending on environmental conditions, notably the presence of oxygen and moisture. Such a decrease of friction by chemically active additives which exhibit poor lubricant action at low temperatures was explained much earlier by Bowden and Tabor (ref. 4) by a chemical reaction leading to the formation of a protective film. However, neither they nor other workers conclusively identified the nature of the film generated by TCP or other lubricants and compared the surface with that outside of the wear track. The changes in profile we found could be explained only in terms of a difference of chemical composition on the surface. Indeed the appearance of the wear track after short failure-free bearing operation is often more likely a manifestation of a chemical change on the surface than of mechanical wear.

In the present study we extended the previous measurements to additives other than TCP and to more operating conditions and developed more sophisticated techniques for the chemical and physical analysis of the surfaces along the wear track. A more conclusive identification of the new metallurgical phase found in the wear track, which was tentatively considered a carbide, was another objective. A high spatial resolution was required since the phase occurred in small patches. In addition to an improved version of the phase-locked interference microscope (PLIM) of our earlier work, an electronic ellipsometer and an Auger electron spectrometer specially adapted for this work were found to be particularly useful.

We want to take this opportunity to thank Dr. Simon Fung for the initial work, Mr. Michael Mailloux for construction of some of the circuitry, and Mr. H. P. Liechti for various improvements in both the PLIM and ESE circuitries. The development of the necessary software was made easier for us by the help of Dr. Dean Chandler-Horowitz from the National Bureau of Standards to whom we hereby express our thanks. Professor Duncan T. Moore of the Institute of Optics, University of Rochester, provided us with most of the knowhow and circuitry of the ellipsometer, for which we are most grateful. Without his continued assistance our ellipsometer would not be built. The Auger analyses were carried out for us by Professor J. B. Hudson of our Materials Engineering Department and we are grateful to him for this work.

MATERIALS

Lubricants

In order to examine the effect of different additives separately and together the same base stock was used with different additives in the same concentrations as in the fully formulated lubricant package. The latter was designed to represent the MIL-L-23699 standard. All lubricants were prepared for us by NASA.

The base stock was the same pure synthesized material, trimethylol propane triheptanoate (TMPTH), used in our earlier study and described in its paper (ref. 2). The lubricants were, in addition to the base stock, solutions in the base stock of

(1) 0.0209 wt % of benzotriazole (BTZ), a corrosion inhibitor,

(2) 1.036 wt % of dioctyldiphenylamine (DODPA), an antioxidant,

(3) 1.036 wt % of phenyl-alpha-naphthylamine (PANA), also an antioxidant,

(4) 2.55 wt % of the antiwear additive tricresylphosphate (TCP), and

(5) all the above additives in the same concentrations together, forming the fully formulated oil, generic MIL-L-23699 (G-MIL-99).

Probe Solution

The probe solution was 0.04 M hydrochloric acid in ethanol.

Bearing Metal

Both components of the experimental ball/plate contact were made of the same alloy steel (M-50) and heat-treated the same way according to the manufacturer's specifications by a local heat treatment company. The (martensitic) steel had the following composition: 0.80 percent carbon, 4.10 percent chromium, 1.00 percent vanadium, and 4.25 percent molybdenum. Its hardness after heat treatment was 62-63 (Rockwell C). The samples were 20.6-mm-diameter balls and 10 by 12 by 3 mm plates, the plate dimensions determined by the inlet system of the scanning Auger spectrometer.

APPARATUS AND EXPERIMENTAL CONDITIONS

Ball/Plate Sliding Contact

In this rig an M-50 bearing ball of 20.6-mm-diameter could be rotated by a horizontal shaft supported by two bearings and driven by an electric motor. The ball was loaded from above by an M-50 plate supported by linear bearings on a horizontal loading platform in such a way that the friction force developed in the contact could be determined from the strain generated in a leaf spring connecting the plate with the loading platform. For this purpose a strain gauge was mounted on the leaf spring and electrically activated in the standard way. The load could be varied by hanging weights on the loading platform. The lubricants were injected into the contact from a reservoir at ambient temperature by a peristaltic pump. No attempt was made to deaerate the lubricants or to control the atmosphere of the contact region.

The maximum Hertzian pressure was 0.1 GPa in all the experiments reported here. The ball speed was 220 rpm, corresponding to 0.2 m/s linear speed. The duration of every run was 30 min at which time the traction force had reached a near-steady value.

No attempt was made to control the contact temperature or to measure it. However, an estimate of the maximum surface temperature rise based on Winer's calculations (ref. 5) indicated that the temperature could have exceeded 220° C, the critical temperature for TCP/surface reaction according to Faut and Wheeler (ref. 3).

AC Phase-Locked Interference Microscope (PLIM)

The instrument (PLIM) (fig. 1) used in this investigation was essentially the same as the one used previously (refs. 1 and 2). It was, however, improved by a superior photo-detector and miscellaneous changes of circuitry. Thus the quality of the reference mirror and vibrational stability are now the major limitations to higher accuracy. At this time ±30 Å in depth and 0.5 μm along the surface plane are the limitations.

It was mentioned earlier that surface profiles measured by the PLIM (or any other optical profilometer) are different from those measured with a stylus profilometer. Since an understanding of this difference is important, a careful analysis of the phenomenon was made. The following brief description should convey the essentials.

Comparison of Optical and Physical Surface Profiles

It will be recalled that any interferometer such as the PLIM compares a reference path length to an unknown length by means of a light beam (laser beam). In our case the distances from the beamsplitter to the vibrating reference mirror and to the surface to be profiled are compared. If the distances are equal or differ by half a wavelength (i.e., a full wavelength of optical path), a bright fringe will be focussed on the detector; if the distances are not equal, a servoloop of the PLIM will apply a voltage to a piezoelectric crystal to move a mirror to make the distances equal and this voltage will be plotted and read in terms of a profile change. However, phases are compared by the laser beam not real distances, for the position of the fringes depend only on phases. Phases are changed on passage through a medium as well as on reflection. Figure 1 gives a schematic drawing of the PLIM, showing the two beams being compared. If a slab of a transparent material (e.g., glass) is introduced into one of the beams, the instrument will record a change even though the surface-to-beamsplitter distance was not changed.

Figure 2 shows the actual situation near the surface to be profiled. The lens fulfills several functions; it focuses the laser beam on a small area, thus giving us spatial resolution and greater brightness, it limits the range of the angle of incidence and it limits the range of the angle of reflection that can return radiation to the PLIM and be detected. Thus angles of incidence and reflection are limited to ±30°. Figure 2 also shows a thin surface layer assumed to be uniform here for simplicity.

A more realistic surface layer is shown in figure 3 in the form of a wedge. The substrate is assumed to be iron, having a complex index of refraction $n_s = 1.5$ to $1.6\,i$. The wedge is assumed to be an iron oxide for which the different indices of refraction shown in the figure have been used in the computation and the 0.1 μm maximum thickness. These values are realistic for bearing surfaces. The top drawing in this figure represents the physical profile of the wedge. The next plot is the optical path difference without taking the phase change on reflection into account. The following plots are those that would be actually recorded: they include both the optical path difference and the phase change on reflection. Clearly the recorded profiles were quite different form the actual physical profile. Different wavelengths

will affect the phase profiles because the complex index of refraction (optical constants) changes with wavelength. The state of polarization of the laser light can also affect the profile.

Our analysis has shown that the thickness of the oxide layer and its optical constants are important factors responsible for the difference between physical and optical profiles. Oxide layers as thin as 0.03 μm or 300 Å can have drastic effects.

Is it possible to deduce the true physical profile from optical profiles? The answer is a qualified yes, if optical profiles have been obtained for different angles of incidence at different wavelengths and perhaps also for different polarizations. In other words, the optical constants (complex indices of refraction) of both film and substrate must be determined from the profile differences. If they are known otherwise, say from ellipsometer data, then the calculations become much simpler. In any case, differences between optical profiles at different wavelengths or between optical and physical profiles are proof of the presence of surface films.

Faraday-Modulated Electronic Recording Scanning Ellipsometer (ESE)

A technique appropriate for the measurement of the thin surface films generated in wear tracks of elastohydrodynamic contacts is ellipsometry. It was necessary to make the ellipsometer spatially scanning and to improve its sensitivity sufficiently to allow identification of the surface materials. Auger electron spectroscopy (AES), which we also used, can also identify surface materials. The justification for having an ellipsometer are: (i) ESE is faster and easier to use than AES since it does not require a vacuum; for the same reason it may also be more realistic, (ii) ESE can supplement AES since it depends on molecular compositions, while AES basically will detect only atomic species, and (iii) ESE can be used directly to measure film thickness, while film thickness measurements by AES require ion milling. On the other hand, ellipsometry is an indirect and less sensitive method of analysis than AES. Clearly it is advantageous to combine ESE with AES.

Since ellipsometry for the study of bearing surface texture was well described by Vorburger and Ludema (ref. 6) and since an extensive article on our ESE will be published elsewhere, only a brief description of our apparatus will be given here. A schematic diagram of the ESE is shown in figure 4. This is the ellipsometer originally designed by Monin and Boutry (ref. 7), which was modified first by Sullo and Moore at the University of Rochester (ref. 8) and now by us. Radiation from the laser source S is polarized by the polarizer P, whose azimuth of vibration with respect to the plane of incidence is θ. On reflection from the sample surface M the plane-polarized radiation has become elliptically polarized. The angle of the semi-major axis of the ellipse and the plane of incidence is γ. CF is a Faraday modulator consisting of a solenoidal coil with a Faraday glass cylinder at its axis. The magnetic field generated by the coil causes the azimuth of polarized radiation of the light traveling along the axis of the cylinder to be changed proportionally to the magnitude of the magnetic field and to the length of the cylinder, the proportionally constant being called the Verdet constant. This phenomenon is known as the Faraday effect. The coil is driven by a 500 Hz oscillator, causing the magnetic field to vary with that frequency.

By the Faraday effect the inclination angle of the polarization ellipse with respect to the plane of incidence is also varied with the same frequency. Monin and Boutry used transmission through a cylinder of water to modulate the elliptically polarized radiation instead of Faraday glass (ytterbium-doped glass). The Faraday glass, having a much larger Verdet coefficient, produces an order of magnitude greater oscillation amplitudes and therefore stronger signals, allowing the ellipsometric analyses of sample areas as small as 100 μm diameter or less. The radiation from the Faraday modulator is passed through the polarization analyzer A of azimuth β and is finally detected by the photocell or photomultiplier PM.

Faraday glass was used by Sullo (ref. 8). Our instrument used two separate Faraday modulators in series instead of the one shown in figure 4. The first modulator contains a 10 cm long, 0.6 cm diameter Faraday glass cylinder (three-times as long as Sullo's) and the second a Faraday glass cylinder of 3 cm length. The current in the first coil is modulated with a 500 Hz frequency, but the current in the second coil is direct current. If the analyzer angle β is equal to the true azimuth γ, the radiation detected at the 500 Hz frequency by phase-sensitive electronic detection is zero and the electronic system is "locked." At the same time the amplitude of the first harmonic (1000 Hz) is monitored to make sure it is nonzero. If, however, the amplitude detected at 500 Hz is nonzero, an error signal is used to add to the DC bias of the second Faraday coil. This adds a DC rotation to the polarization azimuth emerging from the Faraday cells and is equivalent to rotating the analyzer. The direction of the biasing depends on which side of the null the analyzer is at. While the DC bias could be applied to the same coil as the AC, as was done in the Sullo version, having two independent AC and DC coils provides form much greater experimental flexibility and thereby extends the range of the instrument.

Scanning of a sample surface is done by moving the sample M parallel to its plane while recording the corresponding change in DC bias. Thus only the change in azimuth ($\Delta\gamma$) is plotted (the greater portion is set by the analyzer angle β) and the instrument is sensitive to extremely small changes. This, of course, is the main value of electronic detection and scanning.

Thus the method of measurement consists essentially of directing a beam of linearly polarized light at oblique incidence onto the film-covered surface, the thickness and refractive index of the film being determined by analysis of the reflected elliptically polarized beam. The analysis of this elliptical vibration can be carried out in a number of ways, the most commonly adopted one involving the measurement of the parameters Δ and ψ; Δ represents the phase difference between the reflected p and s components vibrating parallel and perpendicular to the plane of incidence respectively, while $\tan\psi$ is the ratio of the reflected amplitudes r_p/r_s. The calculation of Δ and ψ can be done numerically or graphically as shown in figure 5. Sets of θ and ψ are determined for locations on the sample surface by a number of scans at different angles of polarization and plots such as the one of figure 5 are drawn for ever location. The slopes of the γ versus θ curve at $\gamma = 0$, 45, and 90° then provide the values of Δ and ψ. Once Δ and ψ are known, the index of refraction n and the film thickness t can be calculated, but since n is complex, consisting of two variables, more than two measurements are needed, e.g., at more angles of

incidence, (not just at 45°), different wavelengths, etc. The computations can become quite extensive, but are easily performed on a small laboratory computer.

RESULTS

Tractions and Surface Roughness - Effect of the Acid Probe

Figure 6 shows traction curves for the different lubricants after the ball and plates were soaked in them for 3 hr at ambient temperature. These curves are all similar except for the two antioxidants, DODPA and PANA (low final traction) and for the fully formulated oil (high final traction). However, without prior soaking, the traction with TCP was much lower. The operating conditions were such that scoring or scuffing would occur very soon for the fully formulated oil, thereby allowing us to maximize the differences with respect to scoring or scuffing for the additives. From the results, differences between the bearing surfaces for the antioxidants and the TCP without soaking and the other additives could be inferred. To check this idea the surface roughnesses of table I were determined from the optical profiles. The same data were plotted in figure 13. These roughnesses were obtained as follows: A center line was positioned through the optical profile over a distance L in such a way that the sum of the areas under the profile curve above L was equal to the sum of the areas below L. Then roughness was the sum of the areas bounded by L and the profile divided by L times the vertical magnification. The antioxidants DODPA and PANA show the least change over the measured time period within the error limits. DODPA and PANA are also the only lubricants giving a significant reduction of roughness in the initial phase of operation when the acid probe was applied (fig. 7). Since these measurements were made in separate experiments, the consistency of the traction, roughness and acid probe data must be significant. Another interesting observation is the sharp increase in relative roughness change after acid treatment for both BTZ and TCP (fig. 7) in the final stage of the ball/plate run, while the roughness change remained about constant during most of the run.

A closer examination of figure 13 reveals some interesting correlations. Since the vertical scale is arbitrary and the curves were displaced by arbitrary amounts to avoid confusion, only trends are significant. The fully formulated oil (G-MIL-99) and the two amine additives PANA and DODPA gave rise to roughness peaks at about 20 sec. The fully formulated oil, the base oil and BTZ, the anticorrosion additive, had roughness peaks at about 80 sec. Only TCP shows a descending slope beyond 100 sec. These differences might be related to the formation of different surface oxides.

If the additive acted by producing a surface film already on soaking, then one might as well just use the base oil without the additive during bearing operation. This procedure was followed in the experiments that produced the curves of figure 8. Here all the surfaces were soaked for 3 hr in the respective lubricants, cleaned and dried and then immediately used in the traction test with clean base oil. The results are very similar for all lubricants with the notable exception of TCP, which had a much lower traction. BTZ was the next lowest, but the significance of its shift with respect to the others could be questioned. However, BTZ and TCP showed similarity

before (fig. 7). DODPA and PANA and the fully compounded oil had the highest traction force at the end of the experiment.

It will be noted that the curves of figure 8 all slope up while those of figure 7 are mostly flat. The slope is especially high for TCP. This behavior could be ascribed to the removal or change of a surface film or to a change in the surface metallurgy. Just soaking in the additive is inadequate.

Ellipsometry of Wear Tracks

In figure 9 the changes of azimuth with distance across the wear track were plotted. The sample (ball/plate) was soaked in TCP for 3 hr and then run in the ball/plate experiment. Clearly the nature of the surface is different inside the wear track. The change is not caused by a change of reflecting angle for the reflected laser beam is very restricted by apertures. When the angles and corresponding azimuths were changed in order to compute the film thickness and the optical constants, the former came out to be about 60 Å at the maximum and the latter corresponded roughly to Fe_2O_3 by comparison with the data of Leberknight and Lustman (ref. 9). The identification is tentative.

Similar but much smaller changes were found over the wear tracks of the other lubricants containing different additives. The preferential production of a thin oxide layer on wear tracks would seem to be general, but is strongest for those produced in the presence of TCP.

It should be pointed out that the collection of data such as those of figure 9 presents problems different from those encountered when ellipsometry is used with dielectric substrates (ref. 10). Most ellipsometric work today refers to dielectrics and semiconductors. The most important difference is reflectivity -- high for metals and low for dielectrics and semiconductors. Furthermore, metals have a complex index of refraction (two optical constants), dielectrics only a real index of refraction.

Auger Electron Spectroscopy

Since Buckley (ref. 11) presented an excellent review of the technique as it applies to tribology, only the results will be given here.

The plates were analyzed after the ball experiments with every lubricant. Three areas were selected, two within the wear track and one outside for reference. After the experiment, the specimens were washed with alcohol and allowed to dry prior to their introduction into the Auger spectrometer. As a control, a polished unused M-50 plate was included in the set of Auger analyses.

Figure 10 shows an Auger spectrum for a TCP run within the wear scar prior to any treatment within the spectrometer. The principal peaks have been assigned to the elements C, O, Cl, Cr, and Fe. Since C, O, and often Cl are likely surface contaminates, routine ion milling was used. Ion milling was performed with argon ions so that about 10 Å were removed per minute.

After 6 min of ion bombardment the spectrom of figure 11 was obtained. Now most of the C and O were removed and the iron peaks were stronger. The Cl, evidently an impurity, disappeared. At the off-scar position and the same amount of ion bombardment the strengths of the C and O peaks were weaker relative to those of the iron peaks. The Mo and Cr peaks were about of the same strength off-scar and on-scar.

All the other lubricants and the reference gave about the same spectra in the as received condition. However, after 6 min of ion bombardment all the spectra from outside the wear scar as well as from the reference plate were essentially free of O and C while those from inside the wear scar, notably those from TCP and perhaps also from BTZ had a higher O and C content.

In order to show the effect of ion bombardment on elemental composition the plots of figure 12 were drawn for a position within the wear scar. They present the ratios of the O and C peaks to one of the Fe peaks as a function of time. A sharp change of slope after 2 to 4 min probably signifies the removal of a surface layer. The following observations can be made:

(1) All the C-ratios reached a low plateau value after 2 min of ion bombardment (or less). The highest plateau values corresponded to TCP; next was BTZ.

(2) All the C-ratios showed only one change of slope with time of ion bombardment.

(3) All the O-ratios except that of the reference, showed two changes of slope, at 2 and 4 min. After 6 min of ion bombardment, TCP, the fully formulated lubricant (GMIL-99) and BTZ had the highest O-ratio, while the reference had the lowest. Thus there are two O-containing films.

(4) The shapes of the O-ratio plots for TCP and GMIL-99 were similar.

From these observations the following deductions can be made:

(1) The high C-ratios and O-ratios in the outermost surface layer are probably atmospheric contamination.

(2) TCP and GMIL-99 (also containing TCP) have an oxide layer under the atmospheric contamination layer. BTZ is likely to have one as well. The reference, however, does not have such a layer within our error of measurement, but the other materials might have a weak oxide layer.

(3) A carbide layer might also underly the atmospheric contamination layer.

Careful study of the original spectra did not show a higher Cr-concentration in the wear track than without. Buckley (ref. 11) noticed such an increase for 302 stainless steel.

DISCUSSIONS AND CONCLUSIONS

In our previous publications (refs. 1 and 2) the difference in the effect of dilute hydrochloric acid (our acid probe) on causing contour changes within and outside a wear track was described, this difference being especially great when scuffing conditions were approached. It was also found that the presence of the antiwear additive TCP in the lubricant would enhance this difference. Then the question was raised why scuffing could occur so suddenly, apparently without warning, even though operating conditions could have been far from those postulated by the Blok temperature criterion. A principal objective of this study was to try to explain the behavior of the acid probe to help toward arriving at an answer to the above question.

Differences in the optical profile at different wavelengths, ellipsometry and Auger electron spectroscopy have now been shown to discriminate between the surface within the wear track on M-50 steel and outside of it. The evidence points to a higher concentration of an oxide, most likely iron oxide, within the wear track than outside. Interestingly, it appears that TCP promotes the formation of such an oxide. Our Auger spectra never showed phosphorous peaks as others had reported (ref. 12), but then this study used only dilute solutions of TCP while Shafrin (ref. 12) used the pure material. Such an oxide would react much faster chemically with acid than the alloy steel itself. Thus the oxide would explain the behavior of the hydrochloric acid probe. The oxide is more likely to be formed in the wear track than outside of it because of the higher surface temperature in the wear track. It would also reduce friction at higher temperatures, though not at low ones and explain both our data of figure 8 and the results of Faut and Wheeler (ref. 3). Although such an iron oxide layer on the surface could conceivably promote the formation of friction polymer -- whose formation was reported to be enhanced by TCP also -- it is more likely that the same oxidizing conditions that lead to the formation of the oxide also lead to the formation of friction polymer. Since friction polymer is in turn related to acid sludge and the acid is likely to react quickly with the basic iron oxide, provided the temperature is high enough, a case could be made for a mechanism of scuffing, viz. removal of the oxide layer by reaction with acids in the lubricant exposing the nascent metal and allowing metal-to-metal welds. Work now in progress in our laboratory will test this idea.

A new metallurgical phase for M-50 steel was also found and reported in our earlier publication (ref. 2). Its etching characteristics seemed to identify it as a carbide. The higher carbon contents found in the wear track below the surface, especially for TCP, are consistent with this identification.

The sharp initial decrease in the ball experiment of acid probe reactivity of the two amine antioxidants (fig. 7) can be explained by the initial formation of an amine surface film and subsequent exposure of the original alloy steel surface, i.e., the lack of a surface oxide. Since the metal reacts more slowly than the oxide -- which was prevented from forming -- the probe reaction slows down. Once the amine antioxidant is exhausted, the reaction speeds up again, however, thus explaining the increased activity later. The amine surface film could also be instrumental in reducing traction.

The behavior of BTZ, the anticorrosion additive, has been found to be similar to TCP in some ways. Its low oil solubility dictates its low

concentration. By the same token it is more likely to come out of solution and coat the bearing surfaces with an anodic (ref. 13) layer. However, as Parkins (ref. 13) admits, the behavior of these materials is still not well understood.

It would appear that the behavior of TCP with respect to oxide formation in the fully formulated oil is not altered by the other additives as the fully formulated oil behaved similarly. However, there are mutual influences on traction. They should be the subject of further study.

Thus it would seem that leads have been generated to help in the design of lubricating materials to reduce traction and scuffing failure. Their chemical interaction with the bearing surfaces, i.e., the formation of oxide and perhaps other layers is an important key.

REFERENCES

1. Lauer, J. L., and Fung, S. S., "Microscopic Contour Changes of Tribological Surfaces by Chemical and Mechanical Action," ASLE Transactions, Vol. 26, No. 4, Oct. 1983, pp. 430-436.

2. Lauer, J. L., Fung, S. S., and Jones, W. R. Jr., "Topological Reaction Rate Measurements Related to Scuffing," ASLE Transactions, Vol. 27, No. 4, Oct. 1984, pp. 288-294.

3. Faut, O. D., and Wheeler, D. R., "On the Mechanism of Lubrication by Tricresylphosphate (TCP) - The Coefficient of Friction as a Function of Temperature for TCP on M-50 Steel," ASLE Transactions, Vol. 26, No. 3, July 1983, pp. 344-350.

4. Bowden, F. P., and Tabor, D., The Friction and Lubrication of Solids, Oxford, at the Charendon Press, 1964, p. 544.

5. Ausherman, V. K., Nagaraj, H. S., Sanborn, D. M., and Winer, W. O., "Infrared Temperature Mapping in Elastohydrodynamic Lubrication," Journal of Lubrication Technology, Vol. 98, No. 2, April 1976, pp. 236-243.

6. Vorburger, T. V., and Ludema, K. C., "Ellipsometry of Rough Surfaces," Applied Optics, Vol. 19, Feb. 1980, pp. 561-573.

7. Monin, J., and Boutry, G. A., "Concept, Realization and Performance of a New Ellipsometer," Nouvelle Revue d'Optique Appliquee, Vol. 4, No. 3, May-June 1973, pp. 159-169.

8. Sullo, Nancy J., "Measurement of Absolute Refractive Index Profiles in Gradient Index Materials Using Modulation Ellipsometry." M. S. Thesis, Institute of Optics, University of Rochester, 1982.

9. Leberknight, C. E., and Lustman, B., "An Optical Investigation of Oxide Films on Metals," Journal of the Optical Society of America, Vol. 29, No. 2, Feb. 1939, pp. 59-66.

10. Vedam, K., The Characterization of Materials in Research: Ceramics and Polymers, Burke, J. J. and Weiss, V., eds., Syracuse University Press, 1975, pp. 503-537.

11. Buckley, D. H., Surface Effects in Adhesion, Friction, Wear, and Lubrication, Elsevier, Amsterdam, 1981.

12. Shafrin, E. G., and Murday, J. S., "Auger Compositional Analysis of Ball Bearing Steels Reacted with Tricresyl Phosphate," ASLE Transactions Vol. 21, No. 4, Oct. 1978, pp. 329-336.

13. Parkins, R. N.: "Corrosion Inhibition," Electrochemical Materials Science, J. O'M. Bockris, et al., eds., Comprehensive Treatise of Electrochemistry, Vol. 4, Plenum Press, New York, 1981, pp. 307-331.

TABLE 1. - AVERAGE ROUGHNESS[a] OF M-50 BEARING SURFACE AFTER VARIOUS PERIODS OF OPERATING TIME WITH BASE OIL AND BASE OIL CONTAINING VARIOUS ADDITIVES (WITH SOAKING)

	0 sec	10 sec	20 sec	40 sec	1 min	2 min	1 hr
Base oil	245±62	347±72	420±89	448±69	687±148	589±90	645±110
TCP	264±72	246±48	291±88	482±42	460±83	432±56	401±130
DODPA	360±80	306±66	412±52	314±35	308±49	283±26	427±76
PANA	443±74	322±86	459±129	314±45	281±95	349±49	403±67
BTZ	406±150	341±55	271±27	435±62	513±105	318±40	519±126
G-MIL-99	436±35	419±96	598±130	355±152	551±125	296±185	661±227

[a]The average roughness was measured by the centerline average method and the profiles were obtained at 4880 Å wavelength. These data have been plotted in Figure 13.

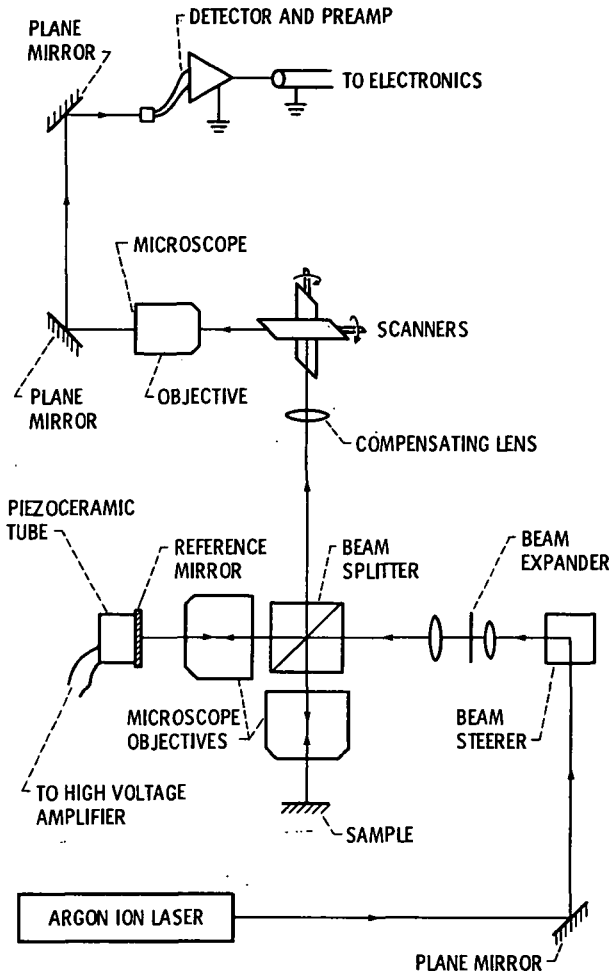

Figure 1. - Schematic drawing of phase-locked interference microscope (PLIM).

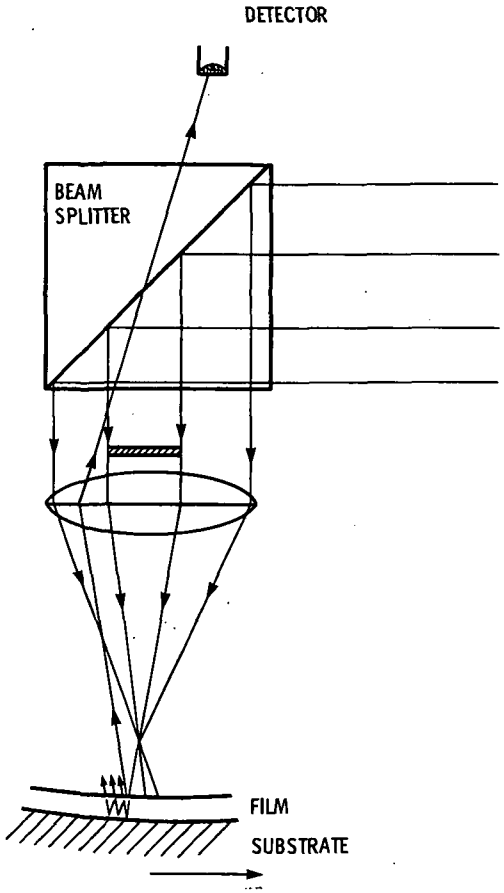

Figure 2. - Close up of light path near sample surface.

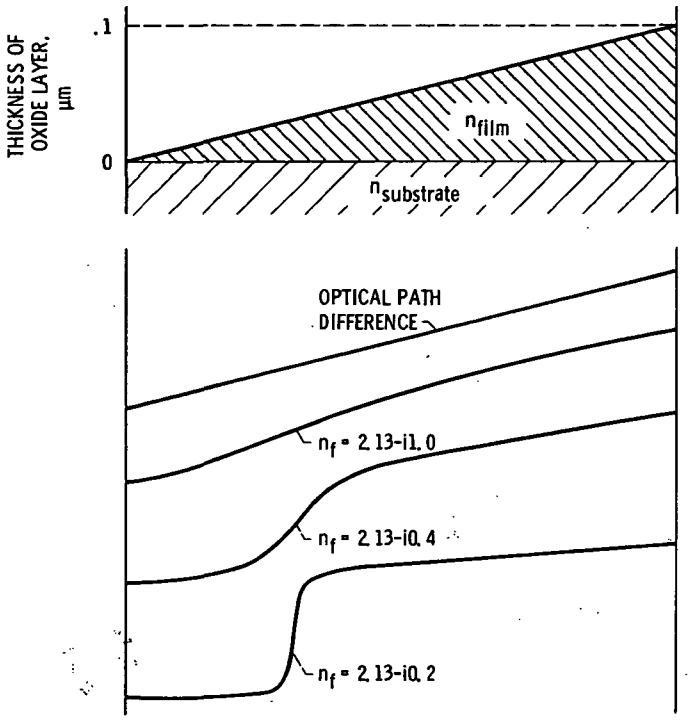

Figure 3. - Comparison of optical and physical profiles. The wedge-shaped iron oxide layer shown at the top can be transformed into the steep step at the bottom by variations of the absorption index.

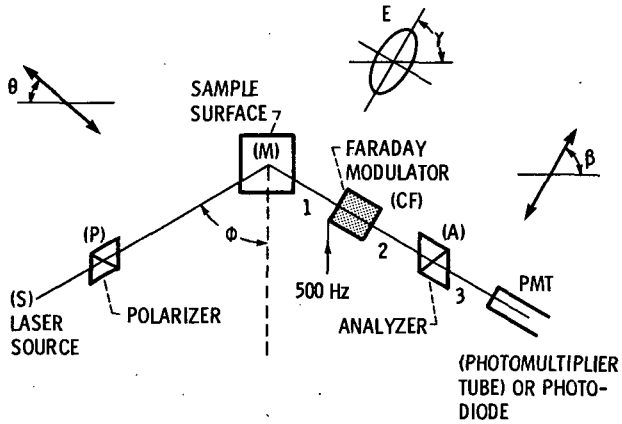

Figure 4. - Schematic drawing of electronic recording scanning ellipsometer (ESE) (ref. 6).

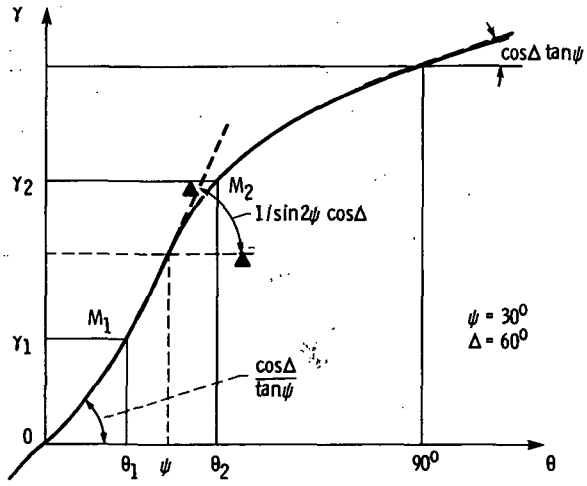

Figure 5. - Determination of the ellipsometer parameters (see discussion in the text; from ref. 6).

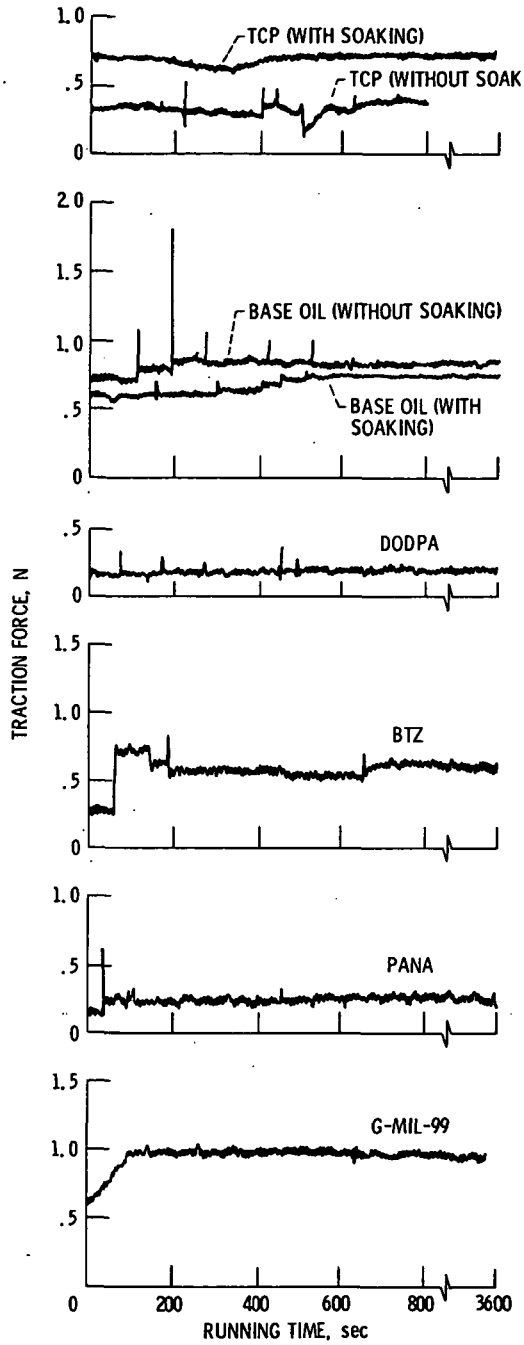

Figure 6. - Traction traces for different lubricants.

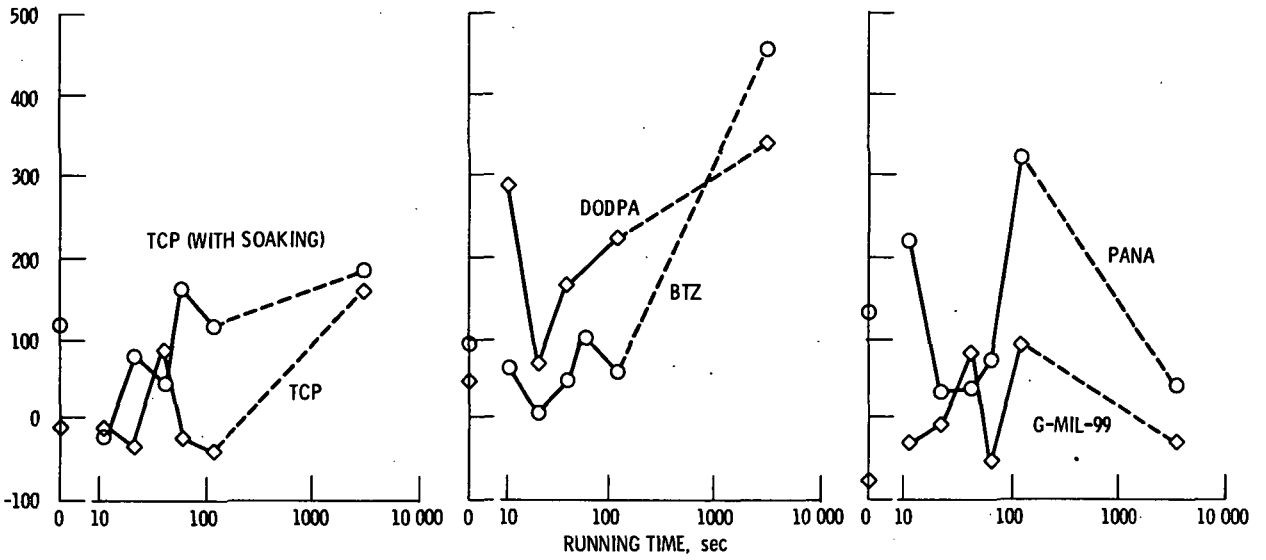

Figure 7. - Effect of acid probe on contact region roughness. (Roughness was measured by the centerline average method and the profiles were obtained at 4880 A wavelength). The relative roughness change is defined as the difference between the roughness before and after acid treatment when roughness itself is defined as the area on the optical profile plot, which is bounded by the center line and the curves above or below for an arbitrary distance.

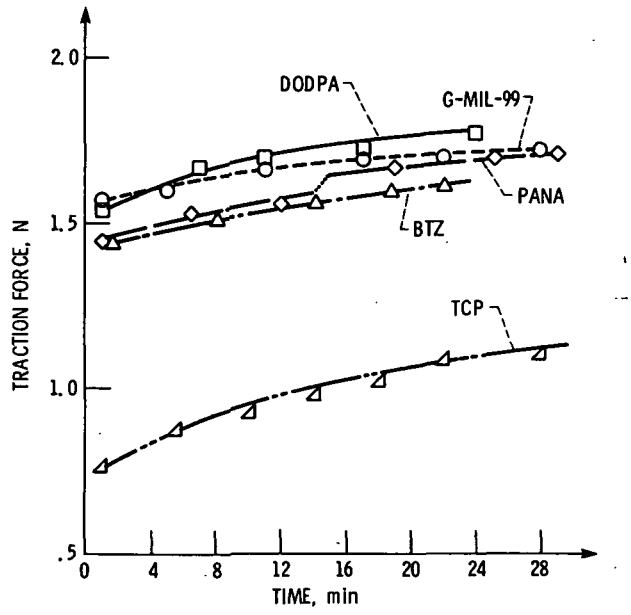

Figure 8. - Traction versus time curves for the base oil after surfaces had been soaked in different additives.

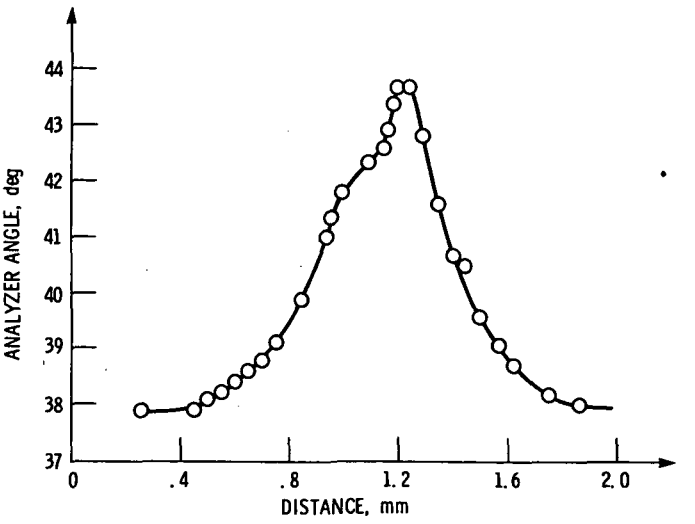

Figure 9. - Ellipsometry trajectory across a wear track produced with TCP in the ball/plate experiment.

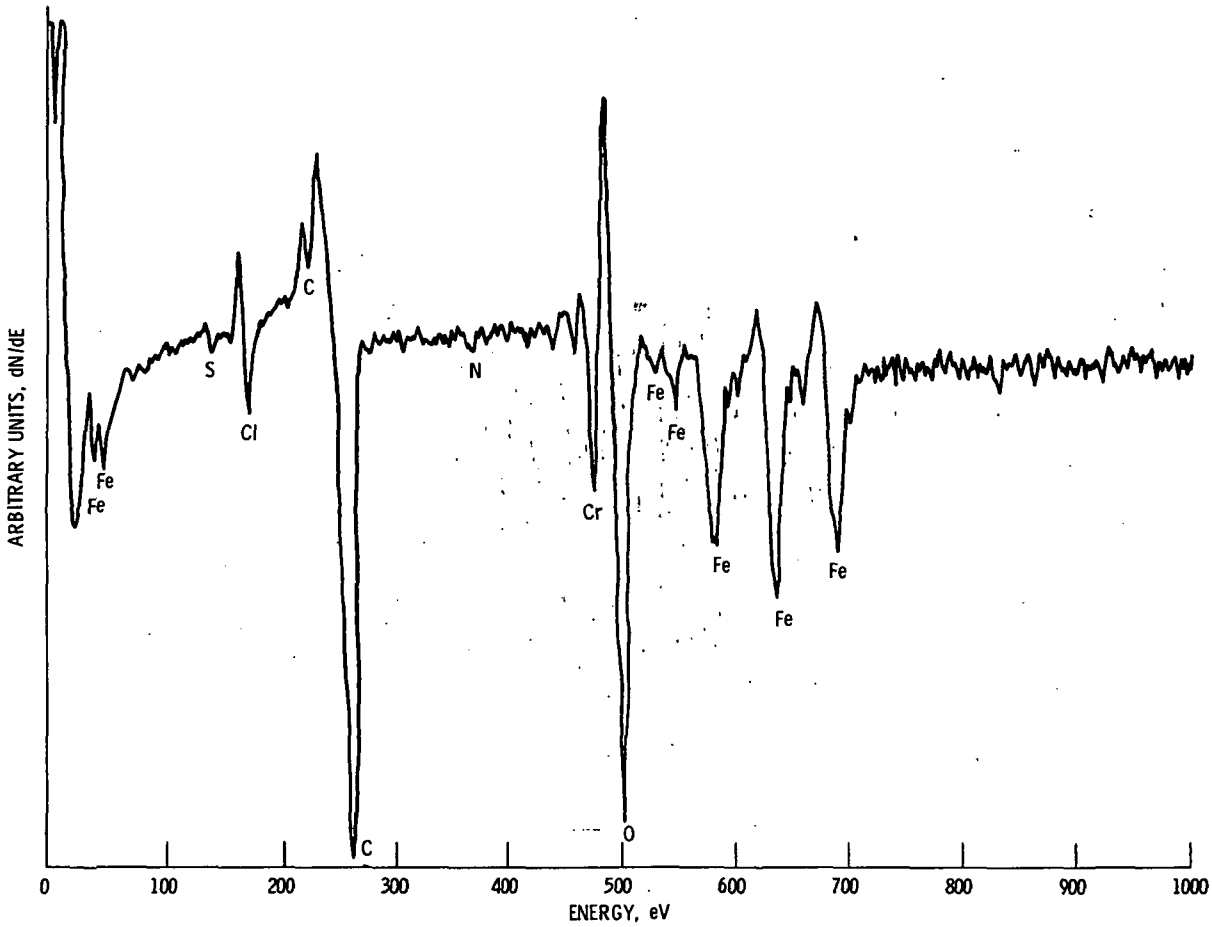

Figure 10. - Derivative Auger spectrum from an area within the wear track produced by the ball experiment with TCP soaking.

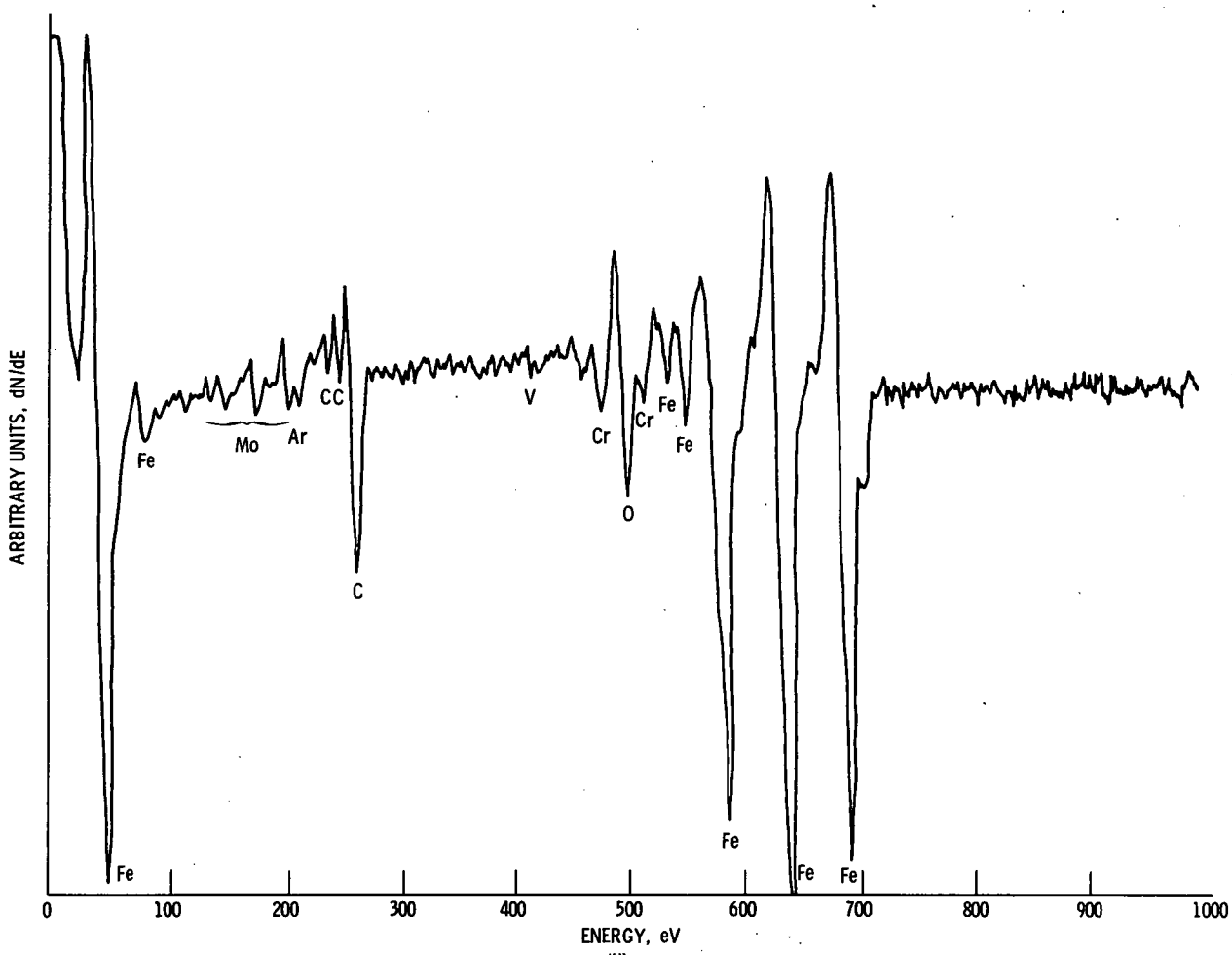

Figure 11. - Derivative Auger spectrum from the figure 10 sample after six minutes of ion bombardment.

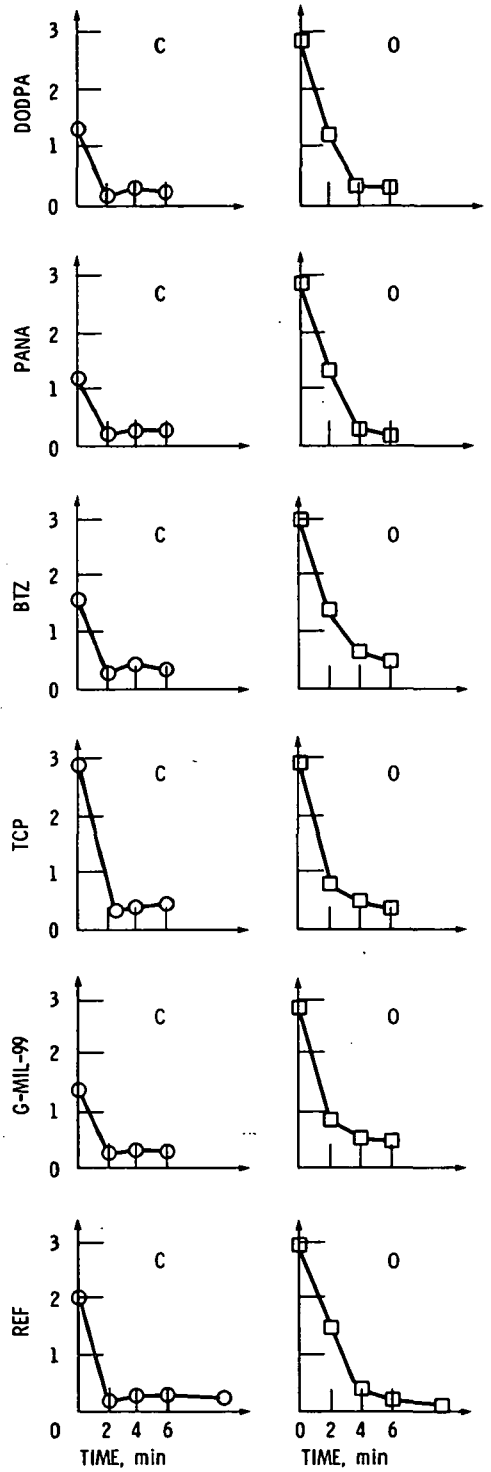

Figure 12. - Ratio of a carbon to an iron Auger peak and of an oxygen peak to the same iron peak for different additives as a function of ion bombardment time. An approximate calibration has shown that about 10 Å of depth are removed in a minute of ion milling. The units of the abscissa are milling time in minutes.

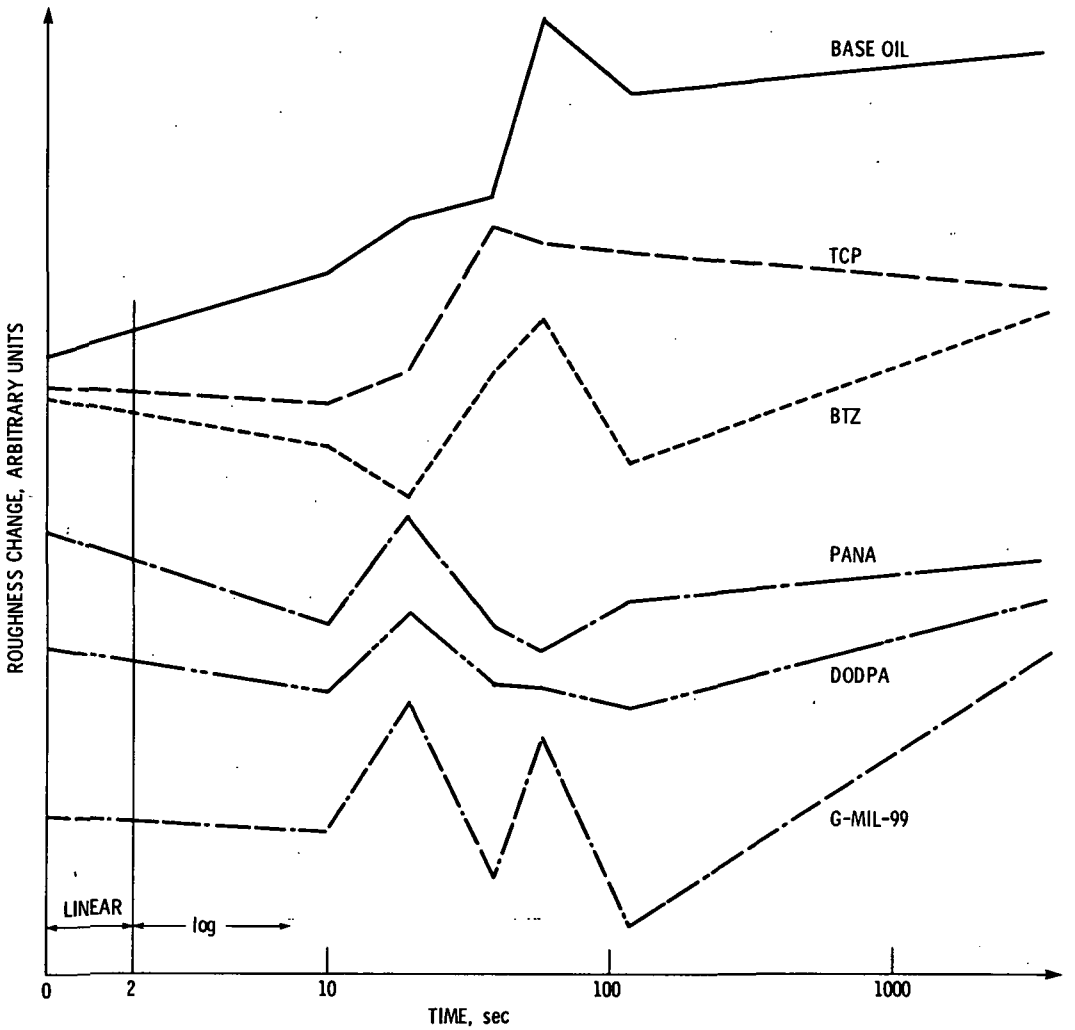

Figure 13. - Roughness changes with operating time of bearing contact. The units of the ordinate are arbitrary, but equal for all the lubricants. The curves for the different lubricants are displaced vertically to reduce confusion. Roughness is defined as the area on the optical profile plot, which is bounded by the center line and the curves above and below for an arbitrary distance.

1. Report No.	2. Government Accession No.	3. Recipient's Catalog No.
NASA TM-83746		

4. Title and Subtitle	5. Report Date
Optical and Other Property Changes of M-50 Bearing Steel Surfaces for Different Lubricants and Additives Prior to Scuffing	6. Performing Organization Code: 505-33-1B

7. Author(s)	8. Performing Organization Report No.
James L. Lauer, Norbert Marxer, and William R. Jones, Jr.	E-2234
	10. Work Unit No.

9. Performing Organization Name and Address	11. Contract or Grant No.
National Aeronautics and Space Administration Lewis Research Center Cleveland, Ohio 44135	13. Type of Report and Period Covered: Technical Memorandum

12. Sponsoring Agency Name and Address	14. Sponsoring Agency Code
National Aeronautics and Space Administration Washington, D.C. 20546	

15. Supplementary Notes: James L. Lauer and Norbert Marxer, Rensselaer Polytechnic Institute, Dept. of Mechanical Engineering Aeronautical Engineering and Mechanics, Troy, New York 12181; William R. Jones, Jr., NASA Lewis Research Center. Prepared for the Joint Lubrication Conference cosponsored by the American Society of Mechanical Engineers and the American Society of Lubrication Engineers, San Diego, California, October 22-24, 1984.

16. Abstract

An ester lubricant base oil containing one or more standard additives to protect against wear, corrosion, and oxidation was used in an experimental ball/plate elastohydrodynamic contact under load and speed conditions such as to induce scuffing failure in short times. Both the ball and the plate were of identically treated M-50 steel. After various periods of operating time the wear track on the plate was examined (i) with an interference microscope of ±30 A depth resolution and (ii) sometimes also with a scanning ellipsometer and (iii) an Auger spectrometer. The optically deduced surface profiles varied with wavelength, indicating the presence of surface coatings, which were confirmed by the other instruments. As scuffing was approached, a thin (~100 A) oxide layer and a carbide layer formed in the wear track in particular when tricresylphosphate antiwear additive was present in the lubricant. The rates of the formation of these layers and their reactivity toward dilute alcoholic HCl depended strongly on the lubricant and additives. Based on these results suggestions for improved formulations and a test method for bearing reliability could be proposed.

17. Key Words (Suggested by Author(s))	18. Distribution Statement
Interference microscope Ellipsometry Auger analysis Scuffing	Unclassified - unlimited STAR Category 27

19. Security Classif. (of this report)	20. Security Classif. (of this page)	21. No. of pages	22. Price*
Unclassified	Unclassified		

*For sale by the National Technical Information Service, Springfield, Virginia 22161

National Aeronautics and
Space Administration

Washington, D.C.
20546

Official Business
Penalty for Private Use, $300

SPECIAL FOURTH CLASS MAIL
BOOK

Postage and Fees Paid
National Aeronautics and
Space Administration
NASA-451

NASA

POSTMASTER: If Undeliverable (Section 158
Postal Manual) Do Not Return